DESIGN TECHNIQUES FOR THE SATURATION MAGNETIC RECORDING PROCESS

By

JOHN POPA

Bachelor of Electrical Engineering

University of Akron

Akron, Ohio

1949

Submitted to the Faculty of the
Graduate College of the
Oklahoma State University
in partial fulfillment of
the requirements for
the Degree of
MASTER OF SCIENCE
May, 1972

DESIGN TECHNIQUES FOR THE SATURATION
MAGNETIC RECORDING PROCESS

Thesis approved:

Paul A. McCallum
Thesis Adviser

Richard L. Cummins

D. Durham
Dean of the Graduate College

PREFACE

A study was undertaken in which design equations were formulated which would enable magnetics system designers to analyze and design magnetic portions of memories for disk storage units.

This work was begun under the sponsorship of the General Electric Company's Memory Equipment Department, Oklahoma City, Oklahoma. The work was continued under the sponsorship of the Honeywell Information System's Peripheral Operations, Oklahoma City, Oklahoma.

My sincere appreciation is extended to the following individuals: Professor P.A. McCollum for serving as my thesis advisor, and Dr. R.L. Cummins for serving patiently these past years as administrator of the off-campus graduate program.

I would also like to thank the management of Honeywell Information Systems Incorporated for allowing me to publish this work. Finally, I wish to thank Mr. L.G. Gitzendanner, who originally supported and encouraged this work; and Mrs. Debbie Parr, for her typing assistance.

TABLE OF CONTENTS

LIST OF TABLES

LIST OF FIGURES

NOMENCLATURE

A	a constant equal to $e(\bar{x})/\psi$, net cross-sectional area of the head core
a	self-demagnetization parameter
B	magnetic flux density
B_R	remenant flux density
C	capacitance, clock pulse
D	denotes a variable
D_1	denotes a variable
d	distance from the head to the media
e	induced voltage
F	farad
f	frequency
G	denotes a variable
g	gap width
H	henries
H_c	coercive force
I	intensity of magnetization of the media
i	current
J	denotes a variable
K	figure of merit for the isolated pulse
L	inductance
$\mathcal{L}$	Laplace transform
ℓ	resultant transition length in the media after

self-demagnetization

M intensity of magnetization of the media (same as I)

m ratio of the self-demagnetization intensity to the coercive force H_c.

N number of turns on the read head

n denotes an integer

P denotes a variable

p pico

Q denotes a variable

R resistance

t time

t_1 minimum reversal time (current or flux)

v voltage drop,
velocity of the media

W track width

x lineal dimension in the x direction

$\bar{x}$ distance from the center of the gap,
velocity · time

α head sensitivity factor,
partial root to quadratic equation

β proportion of the flux emenating from the media which actually links the coil of the head, partial root to quadratic equation

γ type of ferric-oxide

δ media thickness

ϵ 2.71828···

ζ relative amplitude of a given pulse in a pulse train

θ denotes an angle

λ the 50% pulse width of the isolated pulse

μ	permeability of the core material, micro
ν	frequency response of the magnetics system in per unit values
ξ	peak shift in percent of reversal time
π	3.14159 . . .
ρ	denotes a multiplier
σ	denotes a variable
τ	a dummy variable
φ	magnetic lines of flux
Ψ	denotes a constant
Ω	ohms
ω	angular frequency

Subscripts

c	magnetic core parameter
p	parallel parameter
R	remenanent
r	resonant
s	series parameter
x	lineal dimension in the x direction

CHAPTER I

INTRODUCTION

The design of magnetic systems in computer dynamic memory storage devices, such as disk drives or tape drives, requires the availability of design data for data codes, electronic sub-systems, disks or tapes, and magnetic heads. The magnetic system is composed primarily of the magnetic media, (the disk or tape) and the magnetic head. Of equal importance to the design of the system are the characteristics of the write electronics, which together with the head, write the magnetic transitions in the media; and the characteristics of the read electronics, which together with the head, read the electrical data pulses which are stored as magnetic transitions in the media. The coding of the data also influences the design of the magnetics system.

This study provides the magnetics system designer with the techniques necessary to specify the magnetics system after analyzing the effects of the code used, the electronics, and the magnetics. This study considers the saturation magnetic recording process used primarily in the computer industry. Prior to 1968 the primary method of designing the magnetics system of a disc drive was to utilize a code proposed by a communications theory expert,

an electronics system proposed by a data recovery expert, a disk proposed by a disk expert, and a magnetic head proposed by a head expert. This design by committee had obvious faults.

The method put forward in this study represents an extension of the magnetics system concept advocated by Hoagland (1). In the period 1966-1968 the concepts of Hoagland, Speliotis (2), and Morrison (2) were applied. The techniques were not completely satisfactory to a designer because they appeared to lack the continuity required to determine all the magnetics system parameters.

This study was undertaken to translate the concepts of Hoagland, Speliotis, Morrison, and others into design equations and curves. These concepts have been extended to include the state equations of the write process and the read process.

CHAPTER II

LITERATURE SURVEY

The design, and analysis of the magnetics system in a disk drive requires, ultimately, the solution of a set of system equations. Earlier researchers, particularly Hoagland (1) have approached such a solution from an academic point of view. Hoagland provides more of a qualitative insight into magnetic recording than he does of quantitative design information.

Speliotis, and Morrison (2) approach the problem in a manner similar to their contemporaries in the 1960's, but do not consider the problem from a systems point of view. They follow an approach similar to Miyata and Hartel (3) to calculate the demagnetization field in the vicinity of an isolated magnetization transition. From this they determine the extent of the transition region after demagnetization, and the role that the medium thickness, and the magnetic properties of the recording surface play in the resultant magnetization transition. This is characterized by a demagnitization parameter which they call "a". (Middleton (4) also considers this parameter in a manner much more amenable to design techniques.) Speliotis and Morrison continue by calculating the readback signal by the method of images, taking

into account the effect of tape thickness, tape-to-transducer spacing, and read transducer losses. Thus Speliotis, and Morrison define the shape and amplitude of the reproduced pulse in terms of all of the parameters of the magnetic media (tape or disk), and the magnetic head. This equation, although amenable to design techniques, is difficult to handle mathematically when combining pulses into code patterns and pulse trains.

In 1968 the author (5) developed two concepts which helped to develop the needed continuity between the concepts of Hoagland, Speliotis, and Morrison. These two concepts were (a) the representation of the magnetic head by an equivalent circuit, and (b) an approximation to the Speliotis-Morrison equation.

This study establishes the state equations for the write process, and the read process. Thus the write process is represented by a current source (write electronics) driving a load impedance (the magnetic head); and the read process is represented by a voltage source (the magnetic head reading the magnetic storage media) driving a load impedance (read electronics). The digital code is presented to the magnetics system as a current; recovered from the magnetics system as an analog voltage, and the resulting attenuations, peak shifts, distortions, and frequency response are calculated. Once the disk drive specifications are established, the magnetics system designer can specify the disk and the magnetic head by using analytical techniques.

CHAPTER III

DEVELOPMENT OF HEAD EQUIVALENT CIRCUIT

The equivalent circuits for magnetic heads have been derived experimentally by noting the form of the impedance response. Figure 1 shows the impedance response of magnetic heads having different types of magnetic cores.

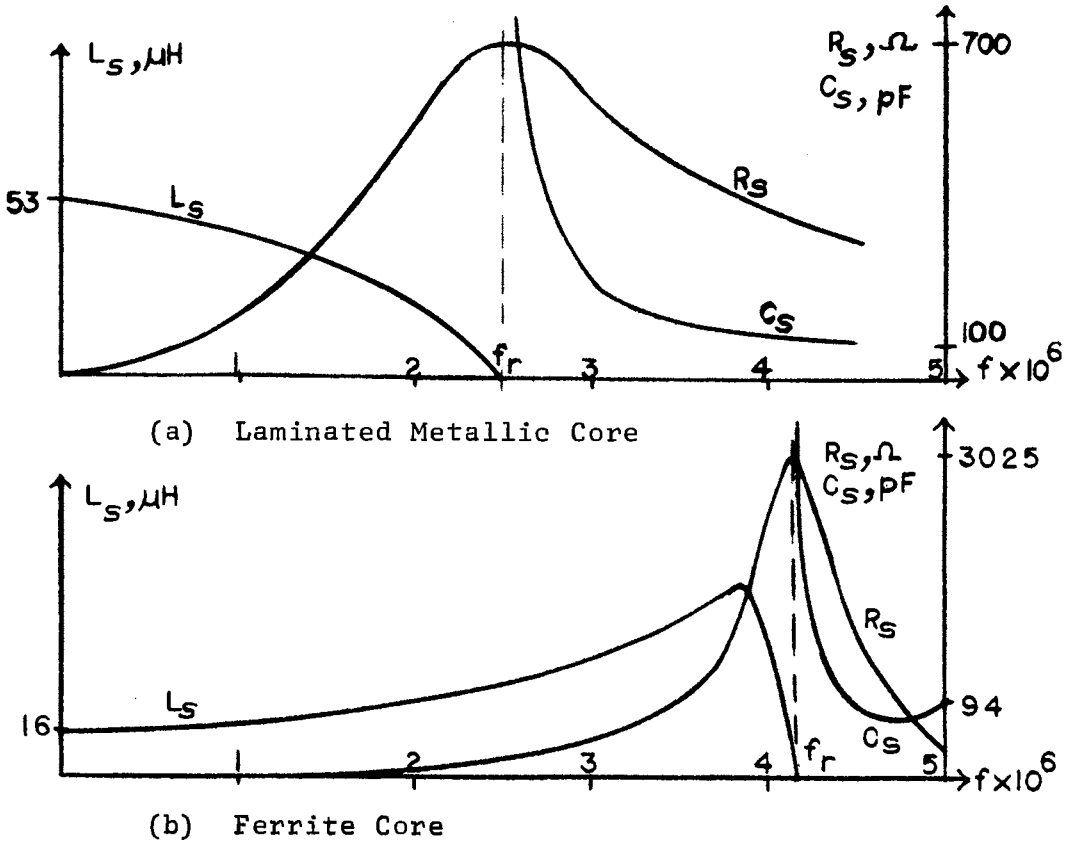

Figure 1. Impedance Response of Magnetic Heads.

These types of response suggest parallel circuits of the form shown in Figure 2.

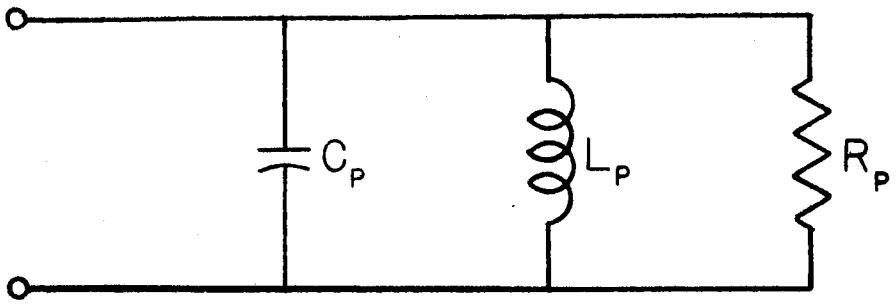

Figure 2. Parallel Circuit Representation of Magnetic Heads.

The series equivalent of this parallel circuit is:

$$R_s + j\omega L_s = \frac{\left(\frac{1}{R_p}\right) - j\left(\omega C_p - \frac{1}{\omega L_p}\right)}{\left(\frac{1}{R_p}\right)^2 + \left(\omega C_p - \frac{1}{\omega L_p}\right)^2} \qquad (3\text{-}1)$$

Resonance is defined as that frequency where:

$$\omega_r C_p = \frac{1}{\omega_r L_p} \qquad (3\text{-}2)$$

Taking the real part of Equation (3-1),

$$R_s = \frac{\left(\frac{1}{R_p}\right)}{\left(\frac{1}{R_p}\right)^2 + \left(\omega C_p - \frac{1}{\omega L_p}\right)^2} \qquad (3\text{-}3)$$

and substituting equation (3-2) into Equation (3-3), at resonance: $R_s = R_p$ (3-4)

Taking the imaginary part of Equation (3-1), and combining terms:

$$L_s = \frac{L_p R_p^2 - \omega^2 L_p^2 R_p^2 C_p}{R_p^2 - 2\omega^2 L_p R_p^2 C_p + \omega^4 L_p^2 R_p^2 C_p^2 + \omega^2 L_p^2} \quad . \qquad (3\text{-}5)$$

Taking the limit of Equation (3-5) as ω approaches zero:

$$\lim_{\omega \to 0} L_s = L_p \qquad (3\text{-}6)$$

From the definition of resonance, Equation (3-2)

$$C_p = \frac{1}{\omega_r^2 L_p} \qquad (3\text{-}7)$$

Thus the lumped parameters of the parallel equivalent circuit are determined from the impedance response of the magnetic head. It will be shown later, in the comparison of experimental results, that the lumped-parameter representation of magnetic heads provides reasonable accuracy over the frequency range of interest.

Most flying magnetic heads employed in disk drives consist of a single, center-tapped coil. Great care is used to make the half coils as nearly identical as possible. It is interesting to note the effects when taking the impedance response of a magnetic head half coil. Since the half coil is assumed to be perfectly coupled to an identical coil during the impedance measurements, Figure 2 can be represented as shown in Figure 3.

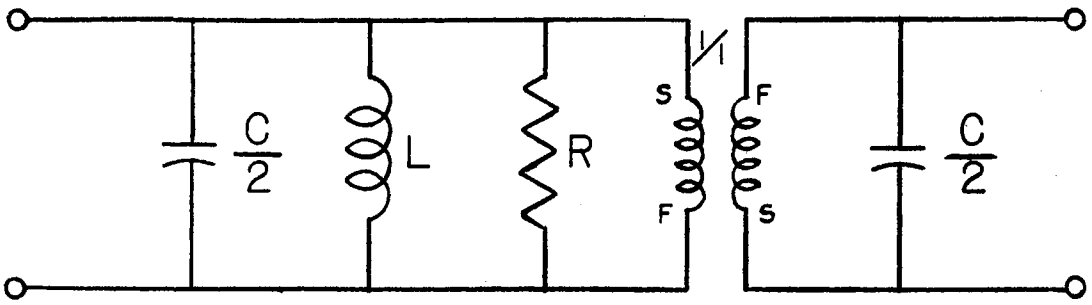

Figure 3. Half Coil Representation of Magnetic Heads.

Figure 3 is the equivalent circuit of a 1:1 ratio transformer with secondary open circuited, and with d.c. resistance and leakage reactance assumed to be negligible. If the primary and secondary are connected in series, the full coil circuit of Figure 4 would evolve.

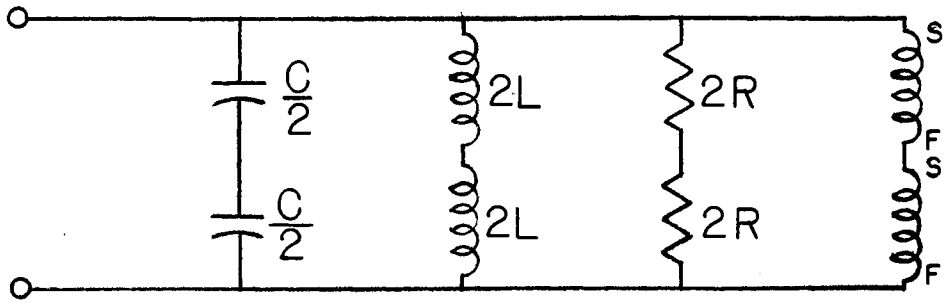

Figure 4. Full Coil Representation of Magnetic Heads.

Combining the elements, the full coil equivalent circuit appears in Figure 5.

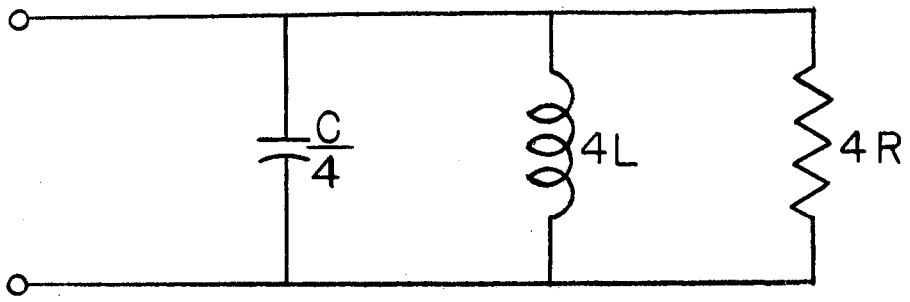

Figure 5. Full Coil Equivalent Circuit.

Substituting the element values of Figures 2 and 5 into Equation (3-2):

$$f_r = \frac{1}{2\pi (LC)^{\frac{1}{2}}} \tag{3-8}$$

for the half coil, and

$$f_r = \frac{1}{2\pi \left[(C/4)(4L) \right]^{\frac{1}{2}}} = \frac{1}{2\pi (LC)^{\frac{1}{2}}} \tag{3-9}$$

for the full coil.

Hence the resonant frequency is the same for a half coil or a full coil. This fact has been observed many times in the laboratory.

In the laboratory it is noted that the elements of a half coil and a full coil are not related by an exact factor of four, although very close to four. This is due to the fact that the leakage reactances were considered negligible, and the coil halves were assumed to be identical in the analysis.

CHAPTER IV

APPROXIMATION TO THE SPELIOTIS-MORRISON EQUATION

Speliotis and Morrison (2) derive the equation for the shape and amplitude of the isolated pulse for the most general case - i.e., the reproduced pulse by a non-ideal ring transducer for a magnetization transition of non-zero width. The derived equation is

$$e(\bar{x}) = \left[Nv\, W\alpha\, (I_R \cdot 10^{-8})\, \frac{4\mu}{\mu+1} \cdot \frac{1}{g} \right] \cdot \left[(\bar{x}+g/2) \ln \frac{(\bar{x}+g/2)^2 + (d+\delta+a)^2}{(\bar{x}+g/2)^2 + (d+a)^2} - (\bar{x}-g/2) \ln \frac{(\bar{x}-g/2)^2 + (d+\delta+a)^2}{(\bar{x}-g/2)^2 + (d+a)^2} + 2(d+\delta+a) \left\{ \tan^{-1} \frac{\bar{x}+g/2}{d+\delta+a} - \tan^{-1} \frac{\bar{x}-g/2}{d+\delta+a} \right\} - 2(d+a) \left\{ \tan^{-1} \frac{\bar{x}+g/2}{d+a} - \tan^{-1} \frac{\bar{x}-g/2}{d+a} \right\} \right] . \quad (4\text{-}1)$$

Equation (4-1) is the most rigorously developed equation for the isolated pulse that has appeared in the recent literature. Unfortunately it suffers from several disadvantages. These disadvantages are:

(1) It is difficult to interpret in a way leading to enhanced insight.

(2) The mathematics involved in combining these pulses into a signal pattern becomes unwieldly.

The disadvantages can be minimized if a relatively simple approximation to Equation (4-1) can be formulated. Such an approximation results as a consequence of determining the self demagnetization parameter, "a".

Middleton (4) following Miyata and Hartel (3) have assumed a transition in the media of the form

$$M_x = (2/\pi) M_R \tan^{-1} (x/a). \qquad (4\text{-}2)$$

The intensity of magnetization M_R can be replaced by the remanent flux density B_R so that

$$B_x = (2/\pi) B_R \tan^{-1} (x/a). \qquad (4\text{-}3)$$

Then

$$B_x/B_R = (2/\pi) \tan^{-1} (x/a). \qquad (4\text{-}4)$$

This function is shown in Figure 6.

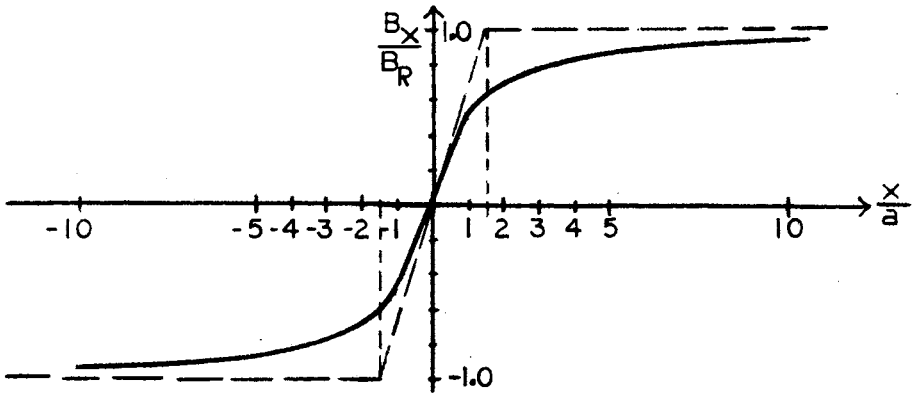

Figure 6. A Magnetic Transition Representation.

The slope of the above function is

$$\frac{d(B_x/B_R)}{d(x/a)} = \frac{2}{\pi}\left[\frac{1}{1+ (x/a)^2}\right] \quad . \tag{4-5}$$

At the origin, the slope is

$$\frac{d(B_x/B_R)}{d(x/a)} = 2/\pi \ ,$$

and $$B_x/B_R \cong (2/\pi)(x/a). \tag{4-6}$$

Extending this line to Saturation ($B_x/B_R = 1$)

$$x = \pi a/2. \tag{4-7}$$

This is the method used by Speliotis and Morrison (2) to define the self demagnetization parameter "a."

Assuming that the resultant transition length written in the media is

$$\mathbf{l} = 2x$$

then $$\mathbf{l} = \pi a \tag{4-8}$$

The voltage induced in a magnetic read head will be of the form

$$e(t) = N \frac{d\phi}{dt} \cdot 10^{-8} \text{ volts.} \tag{4-9}$$

$$d\phi/dt = \beta A_c \, dB/dt \tag{4-10}$$

where β = proportion of the flux emenating from the media which actually links the coil of the head.

A_c = net cross sectional area of the core under the coil.

dB/dt = rate of change of the magnetic transition in the media.

Note that $dB/dt = dB/dx \cdot dx/dt = dB/dx \cdot v$

and from Equation (4-3)

$$dB_x/dx = (2B_R/\pi a)\left[\frac{1}{1 + (vt/a)^2}\right]. \qquad (4\text{-}11)$$

Equation (4-9) can be expressed as

$$e(t) = \frac{2N\beta A_c v \times 10^{-8} B_R}{\pi a}\left[\frac{1}{1 + (vt/a)^2}\right] \qquad (4\text{-}12)$$

Thus it is seen that Equation (4-12) is of the form

$$e(t) = \Psi A\left[\frac{1}{1 + (Kt)^2}\right] \qquad (4\text{-}13)$$

Since Equations (4-13) and (4-1) represent the same isolated pulse, it can be said that Equation (4-13) is an approximation to Equation (4-1). To evaluate the constants Ψ, A, and K,

$$\text{Set } \Psi = \left\{NvW\alpha\,(I_R \cdot 10^{-8})\left[4\mu/(\mu+1)\right] \cdot (1/g)\right\}, \qquad (4\text{-}14)$$

and set $A = \dfrac{e(\bar{x})}{\Psi}$ (4-15)

at t = o.

Then at some later values of t,

($t \geqq 2t_1$ where t_1 equals the minimum value of the flux reversal time)

$$e(\bar{x}_t) \cong \Psi\left[\frac{A}{1 + (Kt)^2}\right]. \qquad (4\text{-}16)$$

$$K = \frac{1}{t}\sqrt{\frac{\Psi A}{e(\bar{x}_t)} - 1}. \qquad (4\text{-}17)$$

The desirability of Equation (4-13) as an approximation to the Speliotis-Morrison Equation (4-1) is enhanced by the fact that Equation (4-13) is easily summed, differentiated, integrated, and the constants are readily evaluated.

CHAPTER V

FREQUENCY DOUBLING METHOD OF DIGITAL MAGNETIC RECORDING

The frequency doubling method of magnetic recording will be reviewed briefly since the design equations to follow have been derived for this system of recording and detection. Figure 7 illustrates the relationship between binary input data, the associated write current, and the read back voltage for a typical binary pattern. A "1" is written by a change in write current at the center of the cell interval, while a "0" would be an absence of a write current change at the center of the cell interval. A "clock" is written by a change in write current at each boundary of the cell.

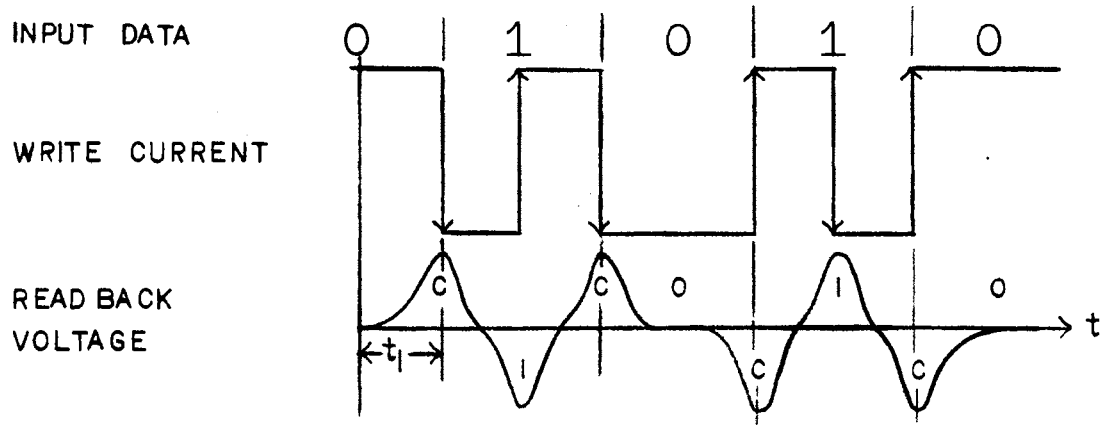

Figure 7. Frequency Doubling Method of Magnetic Recording.

Thus it is seen that the "1's" are written and read back at twice the frequency of the "0's". Since the clock bits have been written into the data stream, the system is known as a self clocking system.

In order to establish a consistent frame of reference for the analyses to follow, the time interval "t_1" will always represent the minimum reversal time (current or flux).

It has been shown in Chapter IV, Equation (4-13), that a mathematical model for an isolated pulse, which can be related back to the parameters of the magnetics system, is

$$e(t) = \Psi A \left[\frac{1}{1 + (Kt)^2} \right] \quad . \qquad (5\text{-}1)$$

With substitution of parameter t_1 in Equation (5-1),

$$e(t) = \Psi A \left\{ \frac{1}{1 + \left[Kt_1 \, (t/t_1) \right]^2} \right\} \quad . \qquad (5\text{-}2)$$

Three observations should be made at this point. The first observation is that the factor K is in reality a figure of merit for the resolution of a magnetics system since each particular system will have a unique value of K. Mathematically, K controls the shape of the pulse and consequently its width. It is shown in appendix A that λ, the 50% pulse width, is

$$\lambda = 2/K \qquad (5\text{-}3)$$

When combining a series of pulses by superposition, K is a measure of the ability to resolve each pulse in the train, and hence a measure of the resolution of the system.

The second observation is that t_1 is a measure of the bit crowding of the system.

The third observation is that any mathematical expression that is a function of Kt_1 is general in nature.

Magnetics Systems Frequency Response

Consider a train of 21 read back pulses as shown in Figure 8.

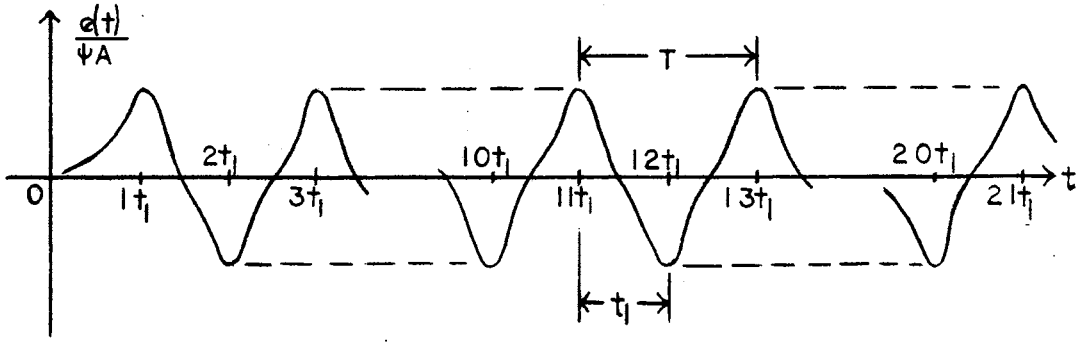

Figure 8. Pulse Train Representation.

Each pulse in the train will be of the form

$$\frac{e(t)}{\Psi A} = \frac{1}{1 + \left[Kt_1 \, (t/t_1) \right]^2} \qquad (5\text{-}4)$$

It is shown in Appendix B that the read back process is a linear process and superposition holds. Hence the train will be of the form

$$\frac{e(t)}{\Psi A} = \frac{1}{1 + \left\{ Kt_1 \left[(t/t_1) - 1 \right] \right\}^2} - \frac{1}{1 + \left\{ Kt_1 \left[(t/t_1) - 2 \right] \right\}^2} +$$

$$+ \frac{1}{1 + \left\{ Kt_1 \left[(t/t_1) - 21 \right] \right\}^2} \qquad (5\text{-}5)$$

In closed form Equation (5-5) can be expressed as

$$\frac{e(t)}{\Psi A} = \sum_{n=1}^{21} \frac{(-1)^{n+1}}{1 + \left\{ Kt_1 \left[(t/t_1) - n \right] \right\}^2} \qquad (5\text{-}6)$$

Figure 8 represents a finite pulse train. To study the frequency response of the magnetics system, a representative pulse is selected at $t=11t_1$ so that the effects of the tails of the preceding and following pulses are included. The relative amplitude is defined to be the ratio of the maximum amplitude of the pulse at $t=11t_1$ to the maximum amplitude of the isolated pulse. The maximum value of the isolated pulse is

$$e_I(t)\max = \Psi A. \qquad (5\text{-}7)$$

The maximum value of the pulse located at $t=11t_1$ is

$$e(11t_1) = \sum_{n=1}^{21} \frac{\Psi A(-1)^{n+1}}{1 + \left\{ Kt_1 \left[11-n \right] \right\}^2} \qquad (5\text{-}8)$$

Dividing Equation (5-8) by Equation (5-7) to obtain the relative amplitude

$$\zeta = \sum_{n=1}^{21} \frac{(-1)^{n+1}}{1 + \left\{ Kt_1 \left[11-n \right] \right\}^2} \qquad (5\text{-}9)$$

It is noted that the relative amplitude is now a function of Kt_1, and can be evaluated for the various degrees of resolution and pulse crowding occurring in double frequency recording. The frequency of the pulse train can be obtained from Figure 8 if it is recognized that the train is an infinite

pulse train as far as the pulse located at $t=11t_1$ is concerned. This is an alternate way of stating that any pulse occurring at negative values of t, and any pulse occurring after $t=21t_1$, will have negligible effects on the pulse occurring at $t=11t_1$. The frequency is

$$f = \frac{1}{2t_1} \tag{5-10}$$

Multiplying numerator and denominator of Equation (5-10) by K and solving for Kt_1

$$Kt_1 = \frac{K}{2f} \tag{5-11}$$

Substituting Equation (5-11) into Equation (5-9) results in an expression relating relative amplitude to frequency. This expression will be called the frequency response of the magnetics system and is given in Equation (5-12)

$$\nu = \sum_{n=1}^{21} \frac{(-1)^{n+1}}{1 + \left[\frac{K}{2f}\left(11-n\right)\right]^2} \tag{5-12}$$

The easiest and most efficient way of solving Equation (5-9) and Equation (5-12) is with the aid of the computer. These two equations are plotted as the curves in Figure 9 and Figure 10.

Peak Shift due to Worst-Case Pattern

The worst case peak shift (both clock and data pulses) in double frequency recording occurs when an isolated "0" is preceded and followed by a string of "1's". For a six-bit train this corresponds to a pattern, 11(10)11.

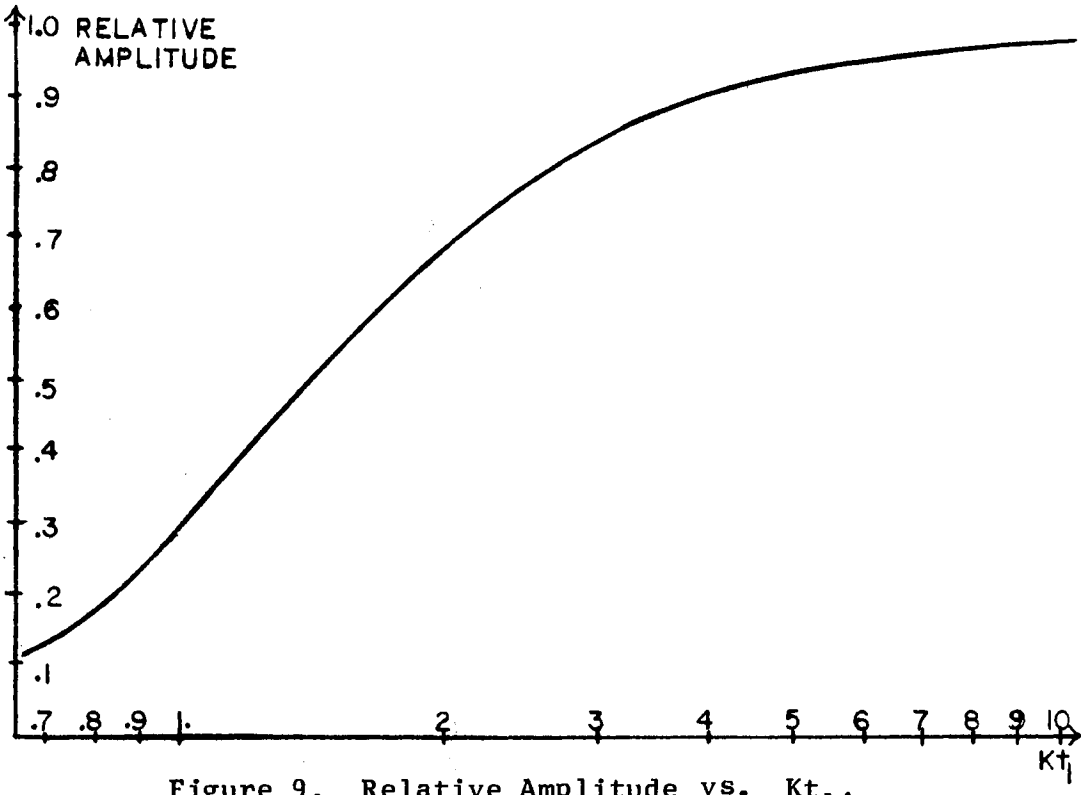

Figure 9. Relative Amplitude vs. Kt_1.

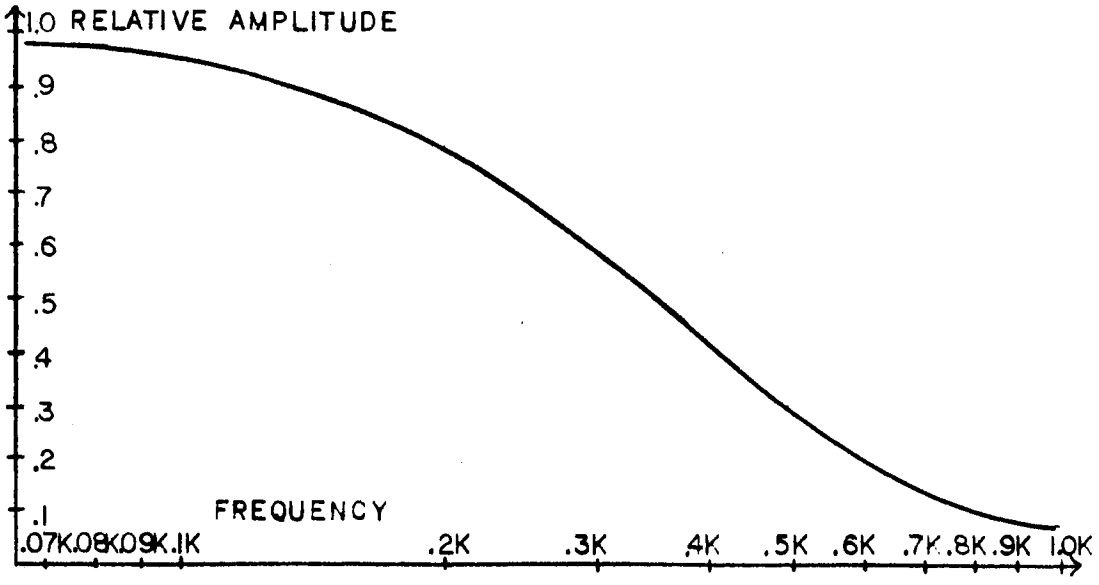

Figure 10. Frequency Response of the Magnetics System.

The circled bits represent the pulses in question. The adjacent pulses (both preceding and following the pulses in question) exert the greatest influence on peak shift. The addition or subtraction of pulses at the beginning or end of a train of six pulses will have very little effect on the center. It is common practice for accuracy in peak-shift analysis to add an identical six-bit train preceding and following the six-bit train in question. It is well to emphasize that the peak shift discussed here is due solely to signal pattern and to the resolution of the magnetics system.

Peak shift (both data and clock pulses) is defined as the deviation of the peaks from the position it should occupy in a symmetrical pulse train. Peak Shift is illustrated in Figure 11.

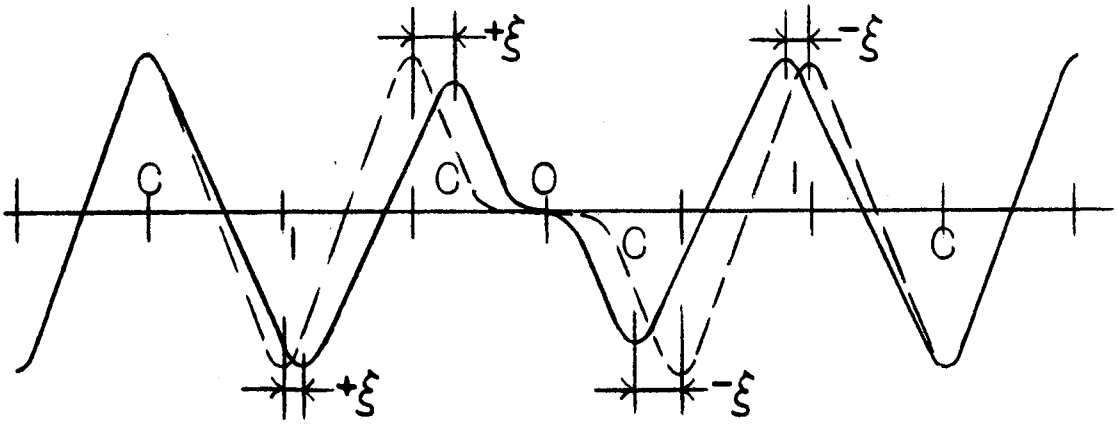

Figure 11. Peak Shift.

It is necessary to construct a mathematical model in order to determine the peak shift for a worst case pattern of 111011

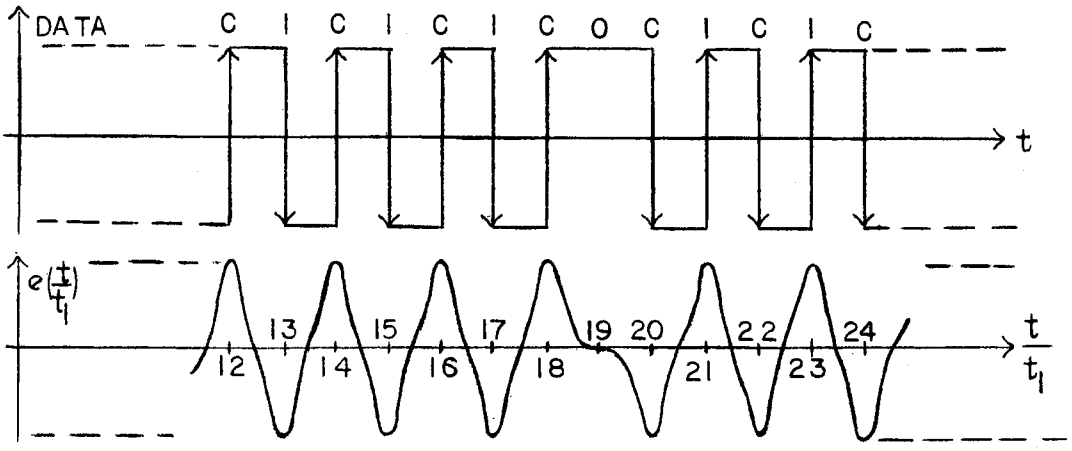

Figure 12. Pulse Train for 111011.

Six identical bits are added before and after the train shown in Figure 12 to insure accuracy of results.

The mathematical model for the total train is

$$e(t) = \Psi A \left[\sum_{n=0}^{6} \frac{(-1)^{n+1}}{1 + \left\{ Kt_1 \left[(t/t_1) - n \right] \right\}^2} + \sum_{n=8}^{18} \frac{(-1)^{n}}{1 + \left\{ Kt_1 \left[(t/t_1) - n \right] \right\}^2} + \sum_{n=20}^{36} \frac{(-1)^{n+1}}{1 + \left\{ Kt_1 \left[(t/t_1) - n \right] \right\}^2} \right] . \qquad (5\text{-}13)$$

Dividing Equation (5-13) by Equation (5-7), the relative amplitude of the train becomes

$$\zeta = \left[\sum_{n=0}^{6} \frac{(-1)^{n+1}}{1 + \left\{ Kt_1 \left[(t/t_1) - n \right] \right\}^2} + \sum_{n=8}^{18} \frac{(-1)^{n}}{1 + \left\{ Kt_1 \left[(t/t_1) - n \right] \right\}^2} + \sum_{n=20}^{36} \frac{(-1)^{n+1}}{1 + \left\{ Kt_1 \left[(t/t_1) - n \right] \right\}^2} \right] . \qquad (5\text{-}14)$$

Equation (5-14) can be solved most efficiently by the use of a computer. It should be noted that the relative amplitude of the train is also a function of Kt_1. Thus Kt_1 will now be termed a magnetics system figure of merit since it influences the amplitudes and peak shifts of any signal combination.

If during the solution of Equation (5-14), the values of t/t_1 are noted at which relative maximums and minimums of $\zeta(Kt_1, t/t_1)$ occur, the peak shifts of each pulse can be determined. Figure 12 shows the unshifted positions of the peaks in question. Equation (5-14) is shown plotted in Figure 13 and curves of peak shift are shown in Figure 14.

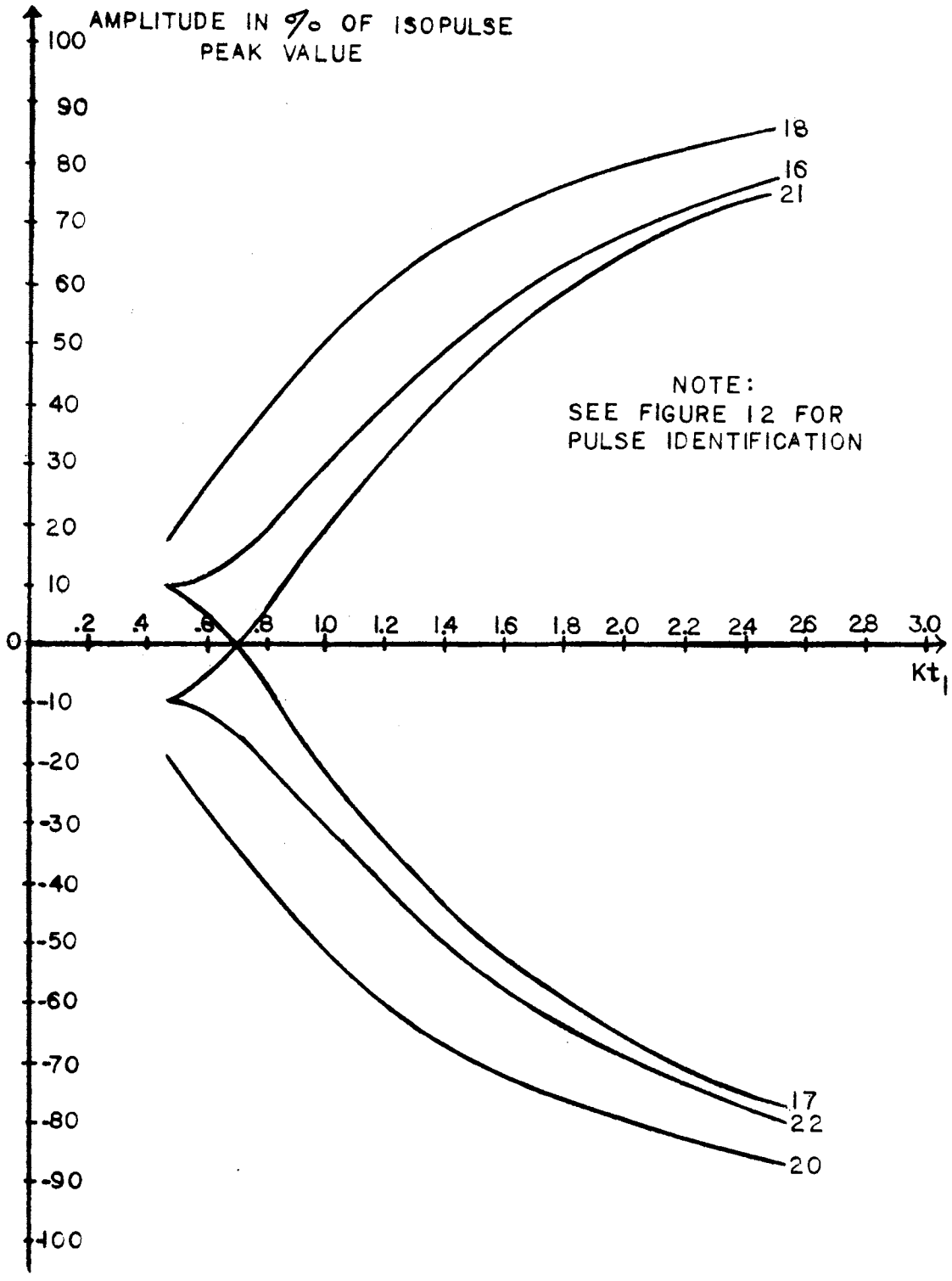

Figure 13. Relative Amplitude of 111011 Pattern vs. Kt_1.

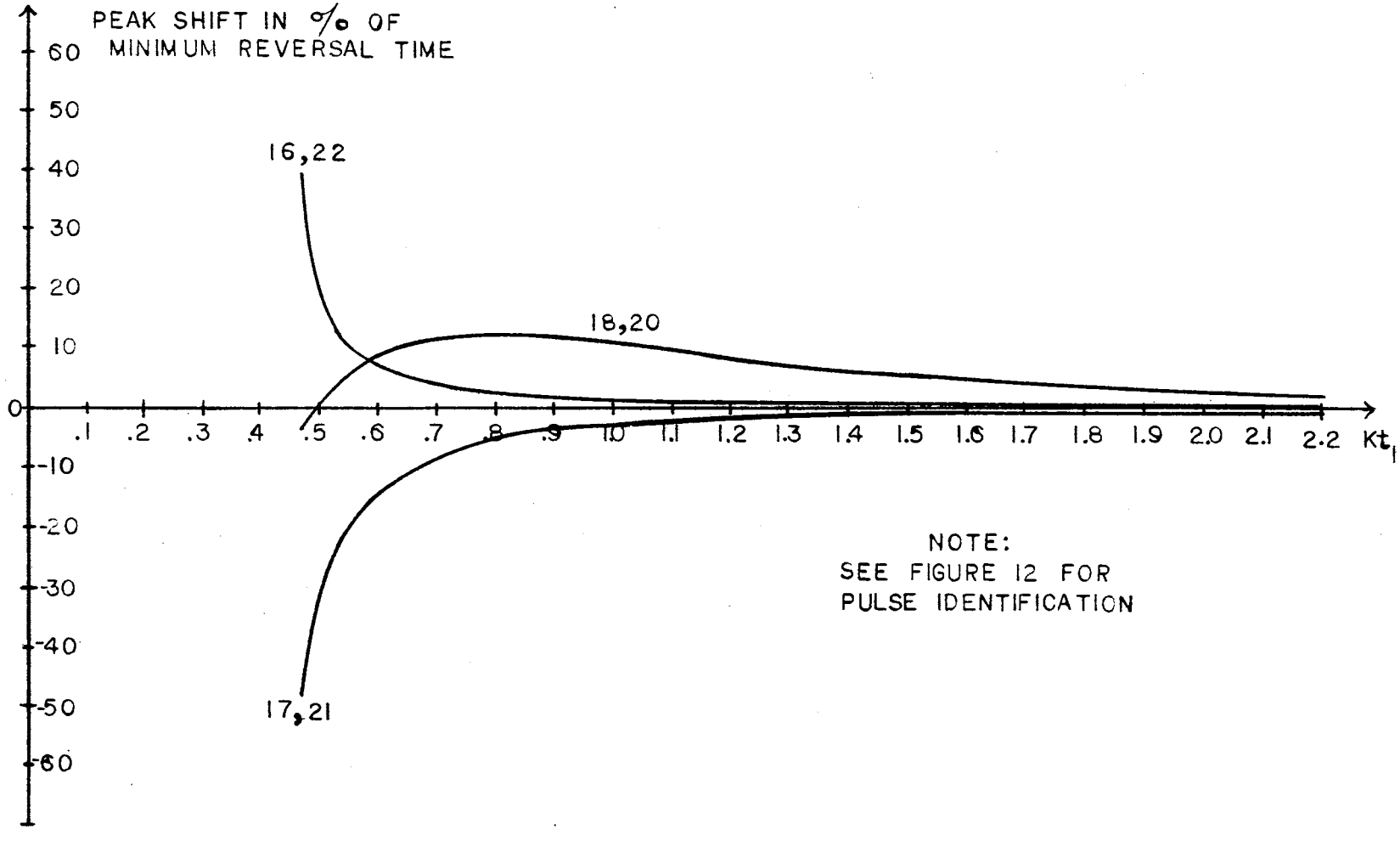

Figure 14. Peak Shift vs. Kt_1.

CHAPTER VI

TRANSIENT RESPONSE

The transient response of a magnetic system can be obtained once the equivalent circuit of a magnetic head is established. The transient response during a write operation is fundamentally different than the transient response during a read operation. The two responses will be treated separately in the discussion to follow.

Write Mode

The rise time of the component of write current which actually produces flux in the core is of particular interest during a reversal of write current. Consider the equivalent circuit of the write mode where i_4 is a current generator representing the write circuit source.

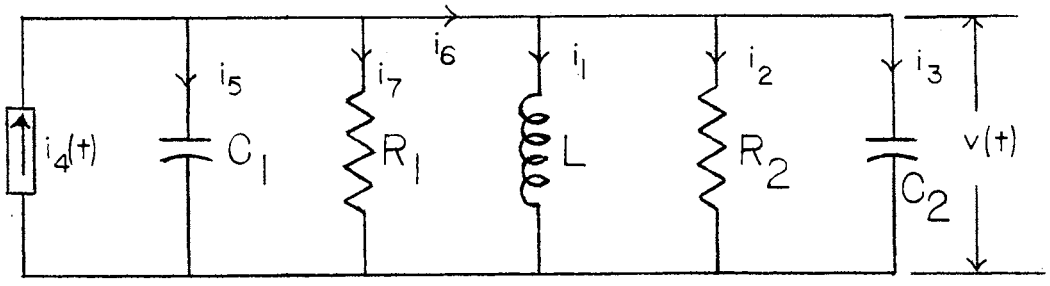

Figure 15. Equivalent Circuit - Write Mode.

$$i_4(t) = -I_4 \mu_1(t) + 2I_4 \sum_{n=1}^{\infty} (-1)^n \mu_1(t-nt_1) \qquad (6\text{-}1)$$

C_1 = write circuit equivalent source and line capacitance

R_1 = write circuit equivalent source and line resistance

L = magnetic head equivalent inductance (half coil)

R_2 = magnetic head equivalent resistance (half coil)

C_2 = magnetic head equivalent capacitance (half coil)

It should be noted that the current i_6 is the only current which can be physically measured in an actual circuit and is sometimes erroneously called the write current. The true write current is the magnetizing current i_1 which produces the flux in the core. (Considerable error can be encountered in rise time measurements if i_6 is taken as the true magnetizing current.) The circuit of Figure 15 can be simplified for analysis by combining the resistances and capacitances as shown in Figure 16.

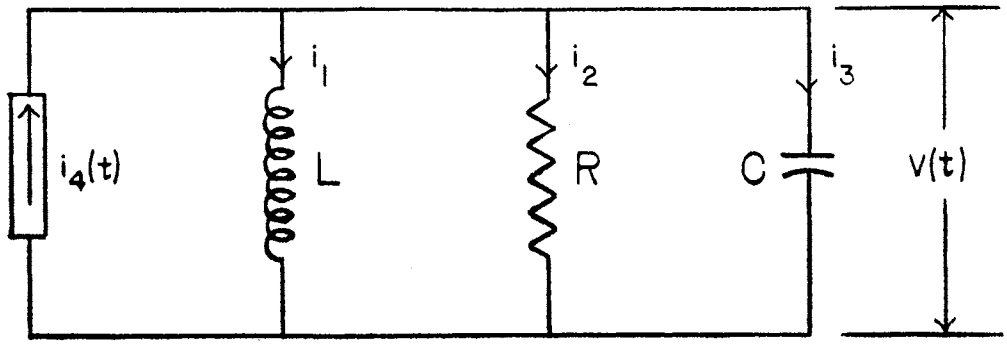

Figure 16. Equivalent Circuit - Write Mode.

$$R = \frac{R_1 R_2}{R_1 + R_2} \tag{6-2}$$

$$C = C_1 + C_2 \tag{6-3}$$

The state equations describing Figure 16 and consequently the write mode are

$$L \frac{di_1}{dt} = v(t) \tag{6-4}$$

and

$$C \frac{dv}{dt} = i_4 - i_1 - \frac{v(t)}{R} \tag{6-5}$$

In normal form the state equations describing the write mode are

$$\frac{d}{dt} \begin{pmatrix} i_1(t) \\ v(t) \end{pmatrix} = \begin{pmatrix} 0 & 1/L \\ -1/C & -1/RC \end{pmatrix} \begin{pmatrix} i_1(t) \\ v(t) \end{pmatrix} + \begin{pmatrix} 0 \\ 1/C \end{pmatrix} i_4(t) \tag{6-6}$$

$$\begin{pmatrix} i_1(t) \\ i_2(t) \\ i_3(t) \end{pmatrix} = \begin{pmatrix} 1 & 0 \\ 0 & 1/R \\ -1 & -1/R \end{pmatrix} \begin{pmatrix} i_1(t) \\ v(t) \end{pmatrix} + \begin{pmatrix} 0 \\ 0 \\ 1 \end{pmatrix} i_4(t) \tag{6-7}$$

Taking the Laplace transforms of the state equations (Equations (6-4), and (6-5)) for a step input of I_4

$$L(sI(s) - I(o)) = V(s) \tag{6-8}$$

$$C(sV(s) - V(o)) = -I(s) - \frac{V(s)}{R} + \frac{I_4}{s} \tag{6-9}$$

Solving Equations (6-8) and (6-9) simultaneously

$$I(s) = \frac{I(o)s^2 + \left[\frac{V(o)}{L} + \frac{I(o)}{RC}\right]s + \frac{I_4}{LC}}{s\left(s^2 + \frac{s}{RC} + \frac{1}{LC}\right)} \qquad (6\text{-}10)$$

$$V(s) = \frac{v(o)s - (1/C)\ (I(o) - I_4)}{s^2 + \frac{s}{RC} + \frac{1}{LC}} \qquad (6\text{-}11)$$

The solution to Equation (6-10) and (6-11) then determines the state of the write mode. The roots to the denominator quadratics of Equations (6-10) and (6-11) are

$$s_{1,2} = -\alpha \pm \beta_1$$

$$\alpha = \frac{1}{2RC} \qquad (6\text{-}12)$$

$$\beta_1 = \left[\left(\frac{1}{2RC}\right)^2 - \frac{1}{LC}\right]^{1/2} \qquad (6\text{-}13)$$

If $\beta_1^2 = 0$, the roots are real and equal and the write system is critically damped.

If $\beta_1^2 > 0$, the roots are real and unequal, and the write system is overdamped.

If $\beta_1^2 < 0$, the roots are imaginary, and the write system is underdamped.

Read Mode

It has been shown in Chapter IV that the isolated pulse is an even function, that is

$$f(-t) \equiv f(t) \quad . \qquad (6\text{-}14)$$

The geometric characteristic of an even function is its symmetry with respect to the vertical axis. It can be shown in the laboratory that the isolated pulse can be made quite asymmetrical about the vertical axis depending upon the manner in which the head is terminated. Thus the transient response of the read mode becomes important in a study of the readback electronics.

Consider the equivalent circuit of the read mode

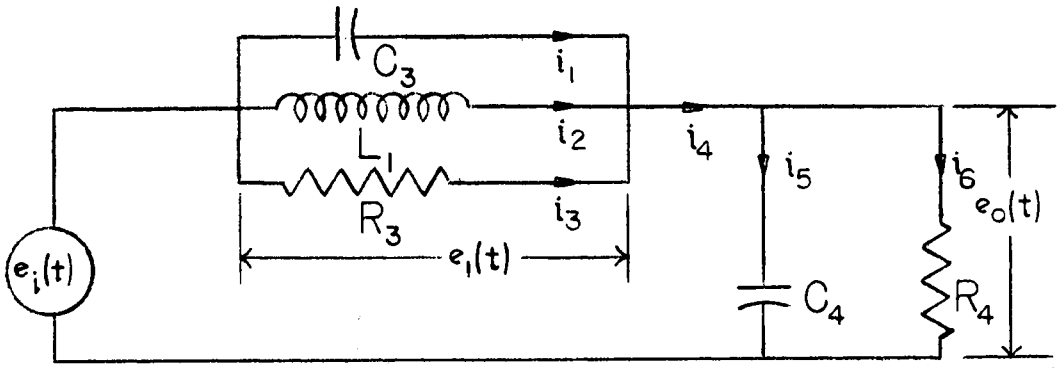

Figure 17. Equivalent Circuit - Read Mode.

where $e_i(t)$ = voltage generator representing the voltage source and having the form

$$e_i(t) = \Psi A \left[\frac{1}{1 + (kt)^2} \right] \qquad (6\text{-}15)$$

L_1 = Magnetic head equivalent inductance (full coil)

R_3 = Magnetic head equivalent resistance (full coil)

C_3 = Magnetic head equivalent capacitance (full coil)

C_4 = equivalent line and preamplifier input capacitance

R_4 = equivalent line and preamplifier input resistance.

The state equations describing Figure 17 and consequently the read mode are

$$\frac{di_2}{dt} = (e_i/L_1) - (e_o/L_1) \tag{6-16}$$

$$\frac{d^2i_2}{dt^2} = \frac{de_o}{dt}\left(\frac{1}{L_1}\right)\left(\frac{C_4}{C_3}\right) - \frac{i_2}{L_1C_3} - \frac{e_1}{L_1R_3C_3} + \left(\frac{1}{L_1R_3C_3} + \frac{1}{L_1R_4C_3}\right)e_o \tag{6-17}$$

Letting $D = \frac{d}{dt}$

$$D^2 = \frac{d^2}{dt^2}$$

$$T_1 = \frac{1}{L_1C_3} \; ; \quad T_2 = \frac{1}{L_1R_3C_3} \; ; \quad T_3 = \frac{1}{L_1R_4C_3}$$

$$T_4 = \frac{1}{L_1}\left(\frac{C_4}{C_3}\right) \; ; \quad T_5 = \frac{1}{L_1} \; ; \quad T_6 = 1/R_4$$

$$T_7 = \frac{L_1}{R_4} \; ; \quad T_8 = C_4 \; ; \quad T_9 = L_1$$

Substituting these values into Equations (6-16) and (6-17)

$$Di_2 = T_5e_i - T_5e_o \tag{6-18}$$

$$D^2i_2 = T_4De_o - T_1i_2 - T_2e_1 + (T_2 + T_3)e_o \; . \tag{6-19}$$

$$\text{Let} \begin{pmatrix} i_2 \\ e_o \end{pmatrix} = \begin{pmatrix} q_1 \\ p_1 \end{pmatrix} \tag{6-20}$$

$$D\begin{pmatrix} i_2 \\ e_o \end{pmatrix} = \begin{pmatrix} q_2 \\ p_2 \end{pmatrix} = D\begin{pmatrix} q_1 \\ p_1 \end{pmatrix} \tag{6-21}$$

$$D^2\begin{pmatrix} i_2 \\ e_o \end{pmatrix} = D\begin{pmatrix} q_2 \\ p_2 \end{pmatrix} \tag{6-22}$$

Substituting Equations (6-20), (6-21), and (6-22) into Equations (6-18) and (6-19),

$$Dq_1 = 0 - T_5p_1 + 0 + 0 + T_5e_i \tag{6-23}$$

$$Dp_1 = 0 + 0 + 0 + p_2 + 0 \tag{6-24}$$

$$Dq_2 = -T_1q_1 + (T_2+T_3)p_1 + 0 + T_4p_2 - T_2e_i \tag{6-25}$$

$$Dp_2 = 0 + 0 + 0 + 0 + 0 . \tag{6-26}$$

In normal form, the state equations become

$$D\begin{pmatrix} q_1 \\ p_1 \\ \hline q_2 \\ p_2 \end{pmatrix} = \left(\begin{array}{cc:cc} 0 & -T_5 & 0 & 0 \\ 0 & 0 & 0 & 1 \\ \hdashline -T_1 & (T_2+T_3) & 0 & T_4 \\ 0 & 0 & 0 & 0 \end{array}\right) \begin{pmatrix} q_1 \\ p_1 \\ \hline q_2 \\ p_2 \end{pmatrix} + \begin{pmatrix} T_5 \\ 0 \\ \hline -T_2 \\ 0 \end{pmatrix} e_i(t) \tag{6-27}$$

$$\begin{pmatrix} i_1(t) \\ i_3(t) \\ i_4(t) \\ i_5(t) \\ i_6(t) \\ e_1(t) \end{pmatrix} = \begin{pmatrix} -1 & T_6 & -T_7 & T_8 \\ 0 & 0 & T_7 & 0 \\ 0 & T_6 & 0 & T_8 \\ 0 & 0 & 0 & T_8 \\ 0 & T_6 & 0 & 0 \\ 0 & 0 & T_9 & 0 \end{pmatrix} \begin{pmatrix} q_1 \\ p_1 \\ q_2 \\ p_2 \end{pmatrix} + \begin{pmatrix} 0 \\ 0 \\ 0 \\ 0 \\ 0 \\ 0 \end{pmatrix} e_i(t) \tag{6-28}$$

The solution of the state equations by conventional techniques can become a formidable task. The response of a linear and relaxed system to an arbitrary excitation can always be found by convoluting the excitation with the impulse response of the system. This is the technique to be employed in the solution of the read mode state equations.

The block diagram of Figure 17 can be represented as follows:

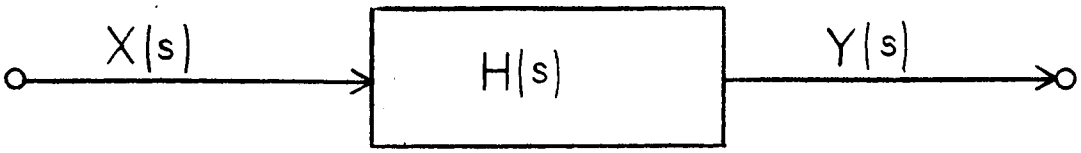

Figure 18. Block Diagram - Read Mode.

If X(s) represents the input to the system, and H(s) represents the system transfer function, then the output is represented by

$$Y(s) = H(s)\ X\ (s)\ . \tag{6-29}$$

From the convolution property of the Laplace transform

$$\int_0^t h(t-\tau)\ x(\tau)\ d\tau = \mathcal{L}^{-1}\left\{ H(s)\ X\ (s) \right\} = y(t). \tag{6-30}$$

Thus the operation to be performed is a graphical convolution of the h (t) and x(t). It is instructive to look at h(t) for a moment. It is the inverse transform of the read mode transfer function. Assume the input to the system is

a unit impulse.

$$x(t) = \delta(t)$$

$$X(s) = \mathcal{L}\left\{\delta(t)\right\} = 1$$

Then $$Y(s) = H(s)\,X(s) = H(s)\cdot 1 = H(s) \qquad (6\text{-}31)$$

$$\mathcal{L}^{-1}\left\{Y(s)\right\} = \mathcal{L}^{-1}\left\{H(s)\right\}$$

$$y(t) = h(t) \qquad (6\text{-}32)$$

Thus the impulse response of a system at rest is equal to the inverse Laplace transform of the system's transfer function. The response of a system to an aribtrary excitation can always be found by convoluting the excitation with the impulse response of the system. For the read mode of Figure 17, Equation (6-30) becomes

$$e_o(t) = \int_o^t h(t-\tau) \cdot \left\{ \frac{\Psi A}{1 + K^2(t-\tau)^2} \right\} d\tau \quad . \qquad (6\text{-}33)$$

The transfer function can be found from a consideration of the impedances in Figure 17.

$$H(s) = \frac{E_o(s)}{E_i(s)} = \frac{a_2 s^2 + a_1 s + a_o}{s^2 + b_1 s + b_o} \qquad (6\text{-}34)$$

where $a_2 = \dfrac{C_3}{C_3 + C_4}$;

$$a_1 = \frac{1}{R_3 (C_3 + C_4)} \quad ; \quad b_1 = \frac{R_3 + R_4}{R_3 R_4 (C_3 + C_4)}$$

$$a_o = \frac{1}{L_1 (C_3 + C_4)} \quad ; \quad b_o = \frac{1}{L_1 (C_3 + C_4)}$$

The roots to the denominator quadratic of Equation (6-34) are

$$s_{1,2} = -\alpha \pm \beta_1$$

$$\alpha = -\frac{b_1}{2} \tag{6-35}$$

$$\beta_1 = \left[\left(\frac{b_1}{2} \right)^2 - b_o \right]^{\frac{1}{2}} \tag{6-36}$$

If $\beta_1^2 = 0$, the roots are real and equal and the transfer function is critically damped.

If $\beta_1^2 > 0$, the roots are real and unequal, and the transfer function is overdamped.

If $\beta_1^2 < 0$, the roots are imaginary, and the transfer function is underdamped.

CHAPTER VII

MEDIA CONSIDERATIONS

Of all the components in the magnetics system, the disk represents the component over which the magnetics system designer has the least control. There are several reasons for this. The range of magnetic properties that can be incorporated into a disk or a disk pack are limited by mechanical considerations. Some of the mechanical considerations are the ability of the media to survive head crashes, the smoothness, flatness, thickness of the surfaces, and the vibration of the surfaces while rotating.

Because of these mechanical problems, and the technology difficulties they produce, it has been common practice in the computer industry to utilize a given disk pack design in more than one generation of disk drive. This then implies that the magnetic properties of the disk are not necessarily optimum in a given design. The design of the magnetics system in this case includes an analysis of the existing disk pack to see if its properties can be utilized.

The Speliotis-Morrison equation can be used for such an analysis. It was pointed out in Chapter IV that Equation (4-13) is much easier to handle mathematically. Using Middleton's (4) equation for "a", and Equation (4-13), it is possible to construct curves which provide magnetics system

performance based upon a disk's characteristics. Middleton's (4) equation states that

$$a = \delta/2 \left[\frac{1}{\tan^2 (m \pi H_c/B_R)} + 1 \right]^{\frac{1}{2}} \qquad (7\text{-}1)$$

For various ratios of H_c/B_R, and a given value of media thickness, it is possible to calculate various values of "a". These values of "a" together with the rest of the magnetics system parameters are inserted into the Speliotis-Morrison Equation (4-1) and the approximation taken as discussed in Chapter IV to yield values of K, and Ψ A. Since K is a figure of merit for the resolution of the magnetics system, and since Ψ A represents the maximum isolated pulse induced voltage, the product KΨA can be viewed as a figure of merit for the media. Figure 19 represents K,ΨA, KΨA as a function of the ratio H_c/B_R for a disk having the following properties.

$$B_R = 400/(H_c/B_R)$$
$$\delta = 110 \times 10^{-6} \text{ inches}$$
$$m = 1$$

It can be seen from Figure 19 that none of the important parameters K,ΨA, and KΨA are maximized at the same value of H_c/B_R. The system designer must then make the decision as to which parameter is most important to his application.

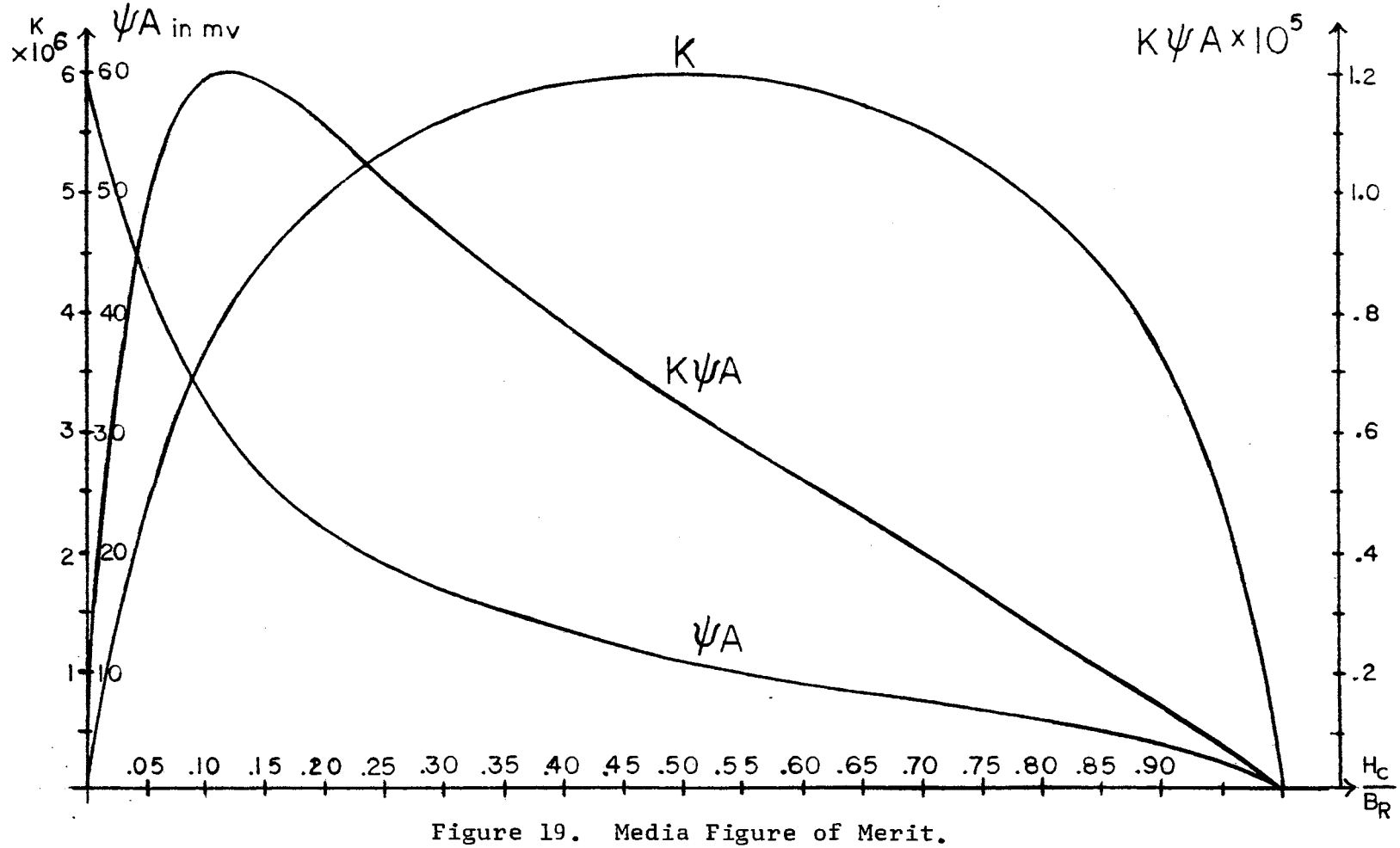

Figure 19. Media Figure of Merit.

CHAPTER VIII

COMPARISON OF RESULTS WITH THEORY AND EXPERIMENT

The results of this study are compared to the theoretical work of Speliotis and Morrison (2) and then to an industry standard disk drive. An industry standard disk drive is a 2200 bit-per-inch device employing frequency doubling coding. The flying heads used in this device are standard ferrite heads and the disk is a standard γ-Fe_2O_3 particulate disk.

Theoretical-Isopulse Equation

The approximate equation for the isolated pulse, Equation (4-13), is compared to the theoretical Speliotis-Morrison Equation (4-1) using the magnetics system parameters for a 2200 bit-per-inch disk drive. The system parameters are:

v=1131 in/sec	N = 80 turns
g=105 x 10^{-6} inches	W = 6.7 x 10^{-3} inches
d=80 x 10^{-6} inches	μ = 1600
δ = 110 x 10^{-6} inches	B_R = 400 gauss
a=77.8 x 10^{-6} inches	Hc = 300 oersteds
	α = .942

A comparison at different points in time is shown in Table I.

TABLE I

COMPARISON OF THE APPROXIMATE ISOPULSE EQUATION TO THE THEORETICAL ISOPULSE EQUATION

Time X 10^{-6} sec.	$[e(t)/\Psi] \times 10^{-4}$ Equation (4-1)	$[e(t)/\Psi] \times 10^{-4}$ Equation (4-13)	% Difference
0	1.0865	1.0865	0
.05	1.0150	1.0148	-.02
.10	.8471	.8470	-.01
.15	.6636	.6640	+.06
.20	.5092	.5098	+.12
.25	.3921	.3926	+.13
.30	.3061	.3065	+.13
.35	.2431	.2434	+.12
.40	.1965	.1967	+.10
.45	.1614	.1615	+.06
.50	.1346	.1346	0
.55	.1137	.1137	0
.60	.0971	.0971	0
.65	.0839	.0839	0
.70	.0731	.0731	0
.75	.0643	.0643	0
.80	.0569	.0569	0
.85	.0507	.0507	0
.90	.0454	.0454	0
.95	.0410	.0410	0
1.00	.0371	.0371	0

The approximate equation differs from the theoretical equation by .13% at the worst point. For the values of system parameters used, the approximate equation is shown to provide an excellent fit to the theoretical equation.

Experimental Results-Head Equivalent Circuit

The impedance response of a metallic, laminated, magnetic head was taken with an impedance bridge. The magnetic head equivalent circuit was determined from these values as

discussed in Chapter III. The resulting values of L,R, and C were then inserted into Equations (3-3) and (3-5) to obtain the theoretical impedance response of the equivalent circuit. The measured values are compared to the calculated equivalent circuit values in Table II.

The same procedure was repeated for a ferrite head and the measured values were compared to the calculated equivalent circuit values in Table III. In both cases the data from the equivalent circuit fits the measured values sufficiently well to conclude that the equivalent circuit selected will provide useful engineering information in the range of operating frequencies.

TABLE II

COMPARISON OF THE EQUIVALENT CIRCUIT IMPEDANCE RESPONSE TO THE MEASURED IMPEDANCE RESPONSE-LAMINATED HEAD-HALF COIL

Frequency x 10^6 Hertz	Measured Values			Equivalent Circuit Values		
	L_s μH	R_s Ohms	C_s pF	L_s μH	R_s Ohms	C_s pF
.2	52	20	-	53	6	-
.4	49	45	-	52	26	-
.6	43	75	-	51	59	-
.8	41	120	-	50	107	-
1.0	39	160	-	48	170	-
1.5	33	345	-	36	388	-
1.8	26	490	-	26	530	-
2.0	22	555	-	18	609	-
2.2	15	620	-	10	665	-
2.4	5	685	-	3	692	-
2.5	0	695	-	0	692	-
3.0	-	590	210	-	635	272
3.2	-	520	160	-	592	202
4.0	-	300	135	-	418	117

TABLE III

COMPARISON OF THE EQUIVALENT CIRCUIT IMPEDANCE
RESPONSE TO THE MEASURED IMPEDANCE
RESPONSE-FERRITE HEAD-
FULL COIL

Frequency	Measured Values			Equivalent Circuit Values		
X10^{6}Hertz	L_s μH	R_s Ohms	Cs pF	L_s μH	R_s Ohms	C_s pF
.5	63	9	-	63	-	-
1.0	64	14	-	66	14	-
1.5	70	35	-	70	38	-
2.0	78	69	-	80	84	-
2.5	91	151	-	96	192	-
3.0	117	388	-	124	471	-
3.5	173	1237	-	186	1656	-
4.0	228	8324	-	210	9008	-
4.16	0	12100	-	0	11858	-
4.3	-	9007	7	-	9483	14
4.5	-	3939	7	-	5409	6
5.0	-	1335	9	-	1402	8

Experimental Results - Write Mode

Measurements were made on the write electronics and a head of a disk drive and the following values were obtained. (Refer to Figure 15)

$R_1 = 218\ \Omega$ $\qquad$ $L = 15.5\ \mu H$

$C_1 = 49.7$ pF $\qquad$ $C_2 = 94.4$ pF

$R_2 = 3025\ \Omega$

combining these values in accordance with Figure 16

$L = 15.5\ \mu H$ $\qquad$ $C = 144.1$ pF

$R = 203\Omega$

Inserting these values into Equation (6-13);

$$\beta_1^2 = -1.543 \times 10^{14} \quad ,$$

and the write circuit is underdamped, or oscillatory. Knowing that the circuit is underdamped, it can be shown that the solutions to the state equations are of the following forms.

$$i_1(t) = I_4 + \epsilon^{-\alpha t} (G \cos\beta t + P \sin \beta t) \qquad (8\text{-}1)$$

$$v(t) = \epsilon^{-\alpha t} (J \cos\beta t - Q \sin\beta t) \qquad (8\text{-}2)$$

where $I_1(o)$ = initial value of current through the inductor

$V(o)$ = initial value of voltage across the inductor

I_4 = generator current

$$\alpha = 1/(2RC)$$

$$\beta = \left\{ \left[1/(LC) \right] - \left[1/(2RC) \right]^2 \right\}^{\frac{1}{2}}$$

$$G = I_1(o) - I_4$$

$$P = (1/\beta) \left[(V(o)/L) + (I_1(o)/RC) - \alpha (I_1(o) + I_4) \right]$$

$$J = V(o)$$

$$Q = (1/\beta) \left[\alpha v(o) + (1/C)(I_1(o) - I_4) \right]$$

Since the generator current is of the form,

$$i_4(t) = -I_4 \mu_1(t) + 2I_4 \sum_{n=1}^{\infty} (-1)^n \mu_1(t - nt_1) \qquad (8\text{-}3)$$

Equations (8-1) and (8-2) can be solved by considering $i_1(nt_1)$ and $v(nt_1)$ at time $t=nt_1$ to be the new initial values, reversing the sign on I_4, and continuing the solution as though a new transient has been initiated.

Equation (8-1) represents the magnetizing current in the head. To find the line current, the state equation can

be solved to yield

$$i_6(t) = i_1(t) + (1/R_2)\ v(t) + C_2 \frac{dv(t)}{dt} \qquad (8\text{-}4)$$

Figure 20 shows the line current and head voltage of a disk drive operating at 2200 bits per inch.

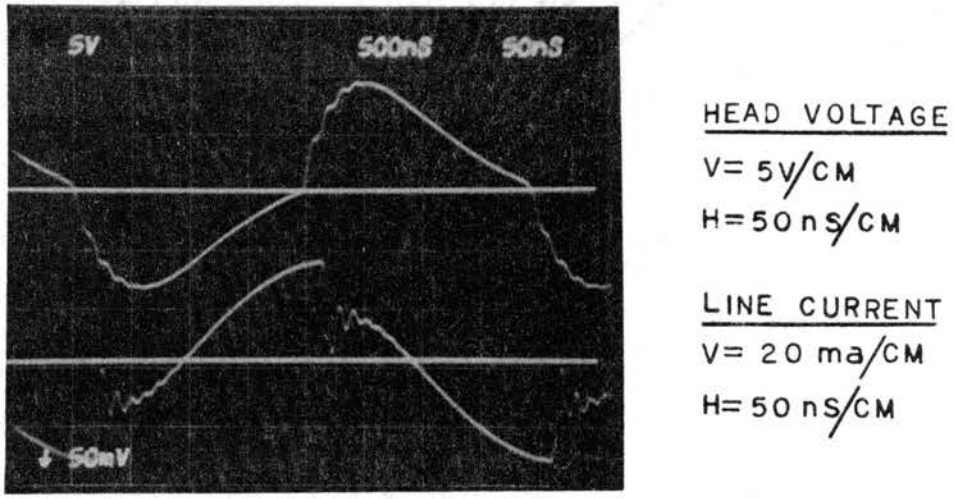

Figure 20. Head Voltage and Line current.

Equations (8-2) and (8-4) are shown plotted in Figure 21. Data points taken from Figure 20 are shown plotted as experimental data on Figure 21. The comparison shows the state equations to be a reasonable representation of the actual circuit in the write mode.

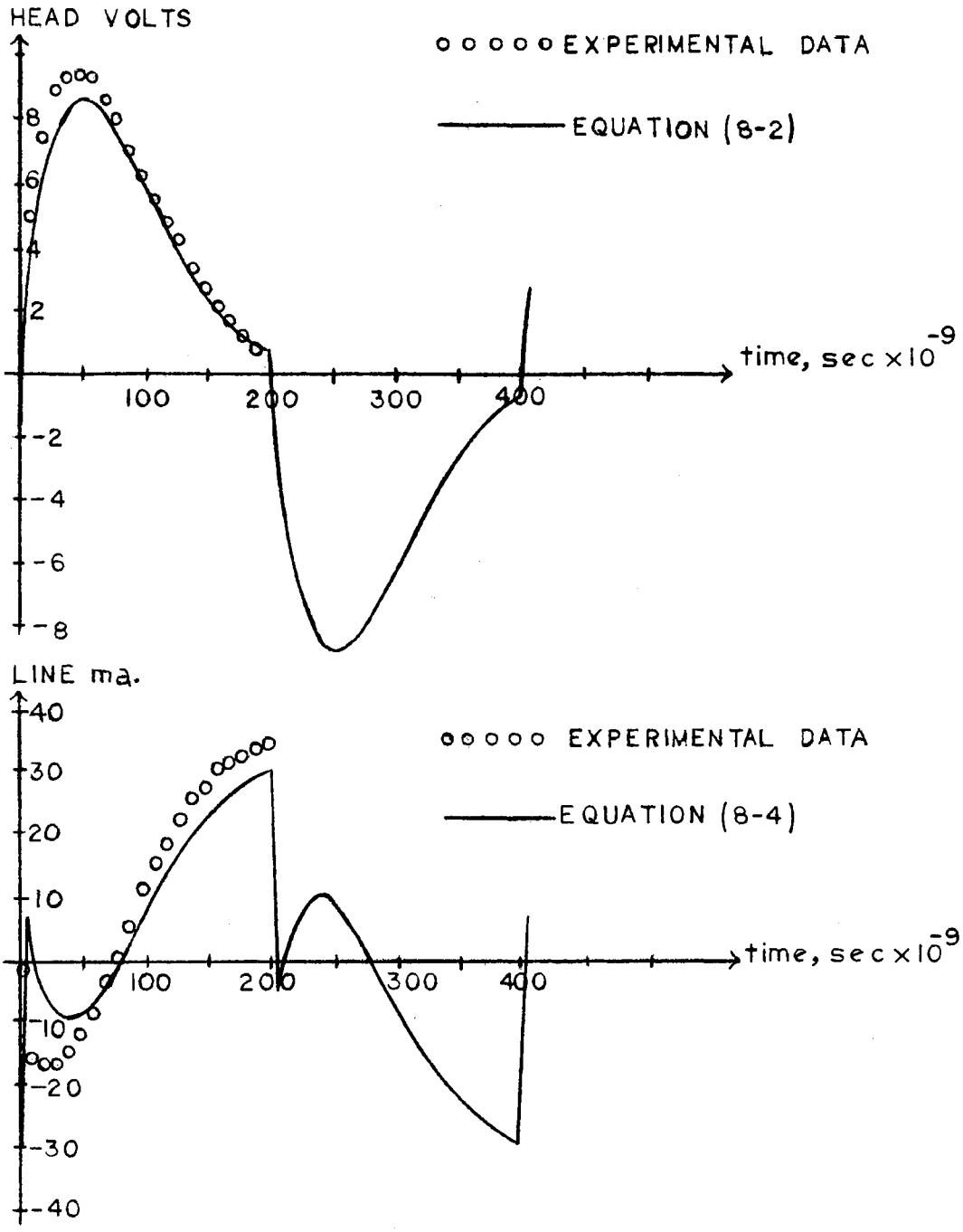

Figure 21. Equivalent Circuit Waveshapes.

Experimental Results - Read Mode

The input impedance of the read electronics and the full-coil impedance values of the magnetic head in the disk storage unit tested were as follows. (Refer to Figure 17.)

$L_1 = 62\mu H$ $\qquad$ $R_4 = 3000\ \Omega$

$R_3 = 12{,}100\ \Omega$ $\qquad$ $C_4 = 20$ pF

$C_3 = 23.6$ pF

Inserting these values into Equation (6-36);

$$\beta_1^2 = -3.471 \times 10^{14},$$

and the transfer function is underdamped, or oscillatory. Knowing that the transfer function is underdamped, it can be shown that the solution to Equation (6-34) is of the following form.

$$h(t) = \left(D_1/\beta \right) \epsilon^{-\alpha t} \sin(\beta t - \theta) \qquad (8\text{-}5)$$

where $D_1 = \left\{ \left[a_2(\alpha^2 - \beta^2) - a_1\alpha + a_o \right]^2 + \left[\beta (2a_2\alpha - a_1) \right]^2 \right\}^{\frac{1}{2}}$

$$\theta = \tan^{-1}\left[\frac{\beta (2a_2\alpha - a_1)}{a_2(\alpha^2 - \beta^2) - a_1\alpha + a_o} \right]$$

and $a_o, a_1, a_2, b_o, b_1, \alpha$, and β_1 are defined in Equations (6-34), (6-35), and (6-36).

Before the convolution defined by Equation (6-33) can be performed, it will be necessary to obtain a value of K. Entering the magnetics system parameters in Equation (4-1) yields a value of $K = 5.32 \times 10^6$. The convolution equation then becomes (on a per unit basis)

$$\frac{e_o(t)}{\Psi A} = \int_o^t h(t-\tau)\, x(\tau)\, d\tau . \qquad (8\text{-}6)$$

where

$$h(t-\tau) = (D1/\beta)\, \exp\left[-\alpha (t-\tau)\right] \sin\left[\beta (t-\tau) - \theta\right]$$

$$x(\tau) = \frac{1}{1 + K^2\left[\tau - (10/K)\right]^2}$$

Equation (8-6) can be solved on a computer, using Gauss' Quadrature Formula as the numerical integration technique(6).

Figure 22 shows the isolated pulse measured on the test disk storage unit

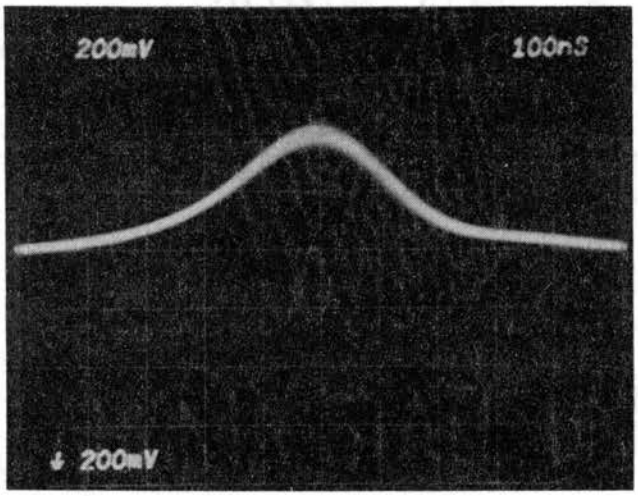

V=200mV/CM

H=100nS/CM

Figure 22. Isolated Pulse - Experimental Result.

The isolated pulse of Figure 22 was measured at the

output of the preamplifier because the input was unavailable for measurements in this particular disk storage unit. Since the exact gain of the preamplifier was unknown, the amplitudes should be viewed on a per-unit basis. The measured value of λ, the 50% pulse width, is seen to be approximately 320 nano-seconds. Since the calculated value of $K=5.32 \times 10^6$ yields a value of λ= 376 nano-seconds (appendix A), a difference between theory and experiment appears to exist. Recall that the calculated value of λ comes from an induced voltage, and the measured value of λ comes from a load voltage. A possible explanation of the difference is the source and load impedance effects.

If a value of $K = 5.7 \times 10^6$, and the magnetics system impedances are entered into Equation (8-6), the graphical convolution of Figure 23 results. The 50% pulse width is measured as 304 nano-seconds. The calculated 50% pulse width corresponding to the K value is 351 nano-seconds. Forming ratios from the values obtained from Figures 22 and 23 yields

$$\frac{\text{unterminated } \lambda}{\text{terminated } \lambda} = \frac{376}{320} = 1.18 \quad (8\text{-}7)$$

$$\frac{\text{unterminated } \lambda}{\text{terminated } \lambda} = \frac{351}{304} = 1.15 \quad (8\text{-}8)$$

Since the ratios are approximately equal, it is concluded that the source and load impedances modify the induced isolated pulse so that it is no longer symmetrical. Data

points taken from Figure 22 are shown plotted as experimental data on Figure 23.

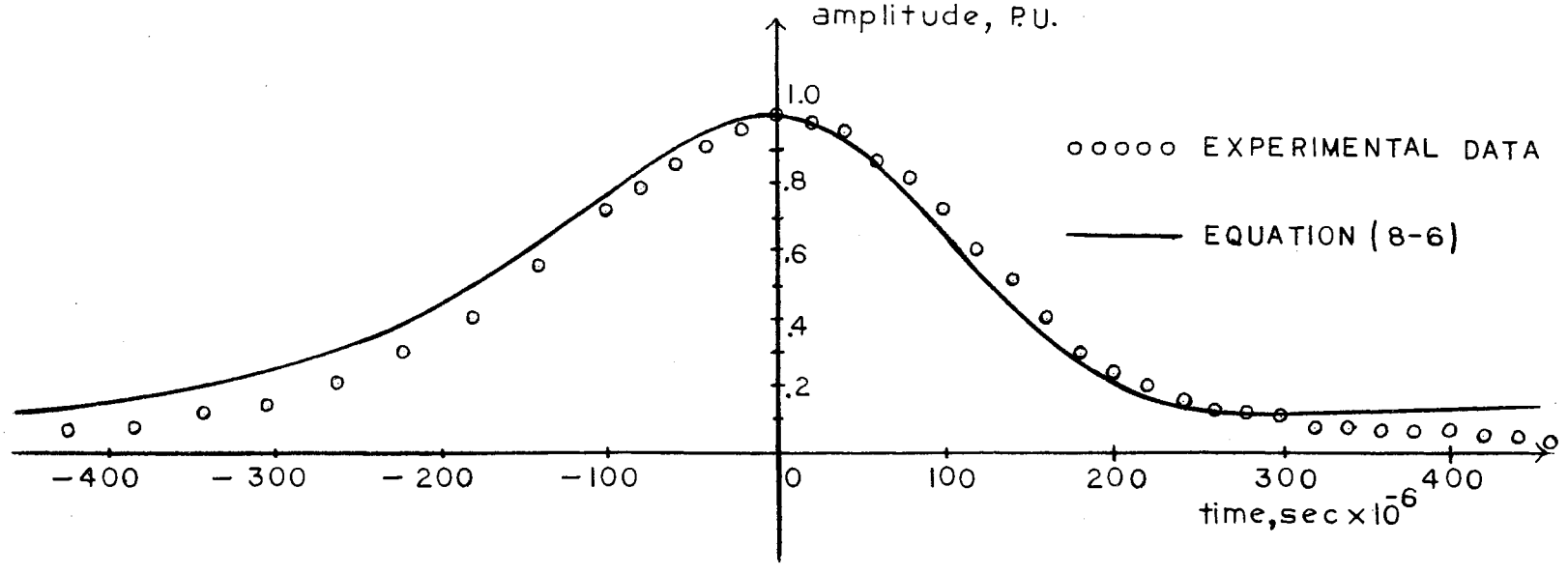

Figure 23. Isolated Pulse - Theoretical Result.

CHAPTER IX

CONCLUSIONS AND RECOMMENDATIONS

Conclusions

(1) The development of the Kt_1 figure of merit allows the design techniques to be general in nature, although the example given is for the frequency doubling method of magnetic recording.

(2) The development of the state equations for the write mode allows an estimate to be made of the magnetizing current and its rise time, although the line current is the only measureable current.

(3) The shape of the readback isolated pulse is not only affected by the magnetics system parameters, but by the electronics terminating the head.

(4) The techniques, curves, and equations described in this study have been used for the past three years in the design and analysis of disk storage units in the engineering laboratories of the General Electric Company's Memory Equipment Department and then at its successor's laboratories, the Honeywell Information Systems Peripheral Operations. The results have shown the design equations to be within the scope of engineering accuracy.

Recommendations

(1) The approach used in this study was to assume that if the rise time of the magnetizing current was shorter than the current reversal time, a proper transition was written in the media. Since the heads in disk storage units do not erase before writing, but simply overwrite any existing transitions in the media, they do not always write a proper transition. This improperly written transition manifests itself as "overwrite" modulation appearing on the readback signal pattern. It is recommended that this "overwrite modulation" problem be studied in greater detail as it is becoming a more serious problem as packing densities (bits per inch) continue to rise in disk storage units.

A SELECTED BIBLIOGRAPHY

(1) Hoagland, A. S. Digital Magnetic Recording, New York: John Wiley & Sons, Inc., 1963.

(2) Speliotis, D. E., and Morrison, J.R. " A Theoretical Analysis of Saturation Magnetic Recording." I.B.M. J. Res. Develop., Vol. 10 (May, 1966), 233-243.

(3) Miyata, J.J., and Hartel, R.R. " The Recording and Reproduction of Signals on Magnetic Medium Using Saturation-Type Recording." I.R.E. Trans. Electron. Comput., Vol. EC-8 (June, 1959), 159-169.

(4) Middleton, B.K. "The Dependence of Recording Characteristics of Thin Metal Tapes on Their Magnetic Properties and on the Replay Head. " I.E.E.E. Trans. Magn., Vol. MAG-2 (Sept., 1966), 225-229.

(5) Popa, J. "Design Techniques for the Saturation Magnetic Recording Process. "G.E. Co. Proj. Memo., 009-506-045 (Oct., 1968)

(6) Scarborough, J.B. Numerical Mathematical Analysis, Baltimore: The Johns Hopkins Press., Sixth Edition, 1966, 152-159.

APPENDIX A

PULSE WIDTH MEASUREMENT

It has been shown in Chapter IV, Equation (4-13) that

$$e(t) = \Psi A \left[\frac{1}{1 + (Kt)^2} \right] \quad . \qquad \text{(A-1)}$$

is an excellent approximation to the Speliotis-Morrison (2) equation. Another advantage of expressing the isolated pulse in the form of Equation (A-1) is that it allows relatively simple experimental verification. If Equation (A-1) is plotted as a function of time.

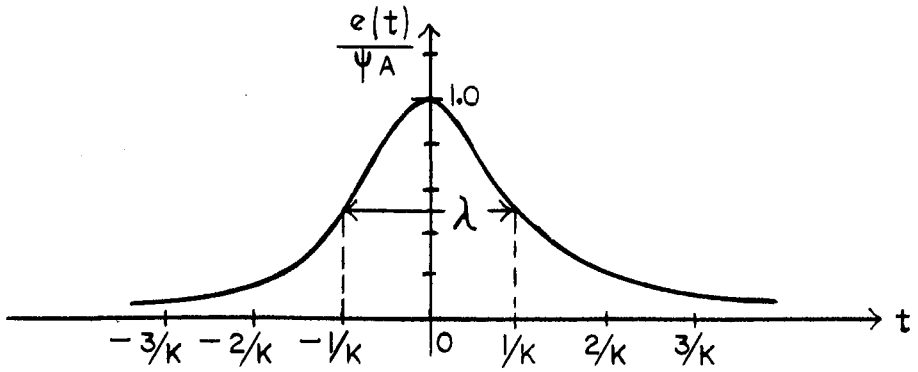

Figure 24. Isolated Pulse - 50% Pulse Width.

The 50% amplitude occurs at

$$\frac{e(t)}{\Psi A} = .5 = \frac{1}{1 + (Kt)^2}$$

$$Kt = \pm 1$$

$$t = \pm 1/K$$

If λ is defined as the width of the isolated pulse at the 50% amplitude points

$$\lambda = \Delta t = 1/K-(-1/K)=2/K \text{ seconds.} \qquad \text{(A-2)}$$

Thus a simple and accurate way of evaluating the resolution figure of merit K, is to measure the 50% pulse width of the isolated pulse (in seconds) and apply Equation (A-2)

$$K = 2/\lambda$$

APPENDIX B

SUPERPOSITION - LINEAR SYSTEMS

A magnetic read system can be considered a summing device which sums the voltages induced in the head by the individual magnetic transitions written into the media. The input-output relation is

$$y = H \begin{bmatrix} +e_1 \\ -e_2 \\ +e_3 \\ \cdot \\ \cdot \\ \pm e_n \end{bmatrix} = e_1 - e_2 + e_3 - \cdots \pm e_n \qquad \text{(B-1)}$$

The magnetic read system exhibits the property of additivity since

$$y = H\rho \begin{bmatrix} +e_1 \\ -e_2 \\ +e_3 \\ \cdot \\ \cdot \\ \pm e_n \end{bmatrix} = H \begin{bmatrix} +\rho e_1 \\ -\rho e_2 \\ +\rho e_3 \\ \cdot \\ \cdot \\ \pm \rho e_n \end{bmatrix} = \rho e_1 - \rho e_2 + \rho e_3 - \cdots \pm \rho e_n \qquad \text{(B-2)}$$

The magnetic read system also exhibits the property of homogeneity since

$$y = H\rho \begin{bmatrix} +e_1 \\ -e_2 \\ +e_3 \\ \cdot \\ \pm e_n \end{bmatrix} = H \begin{bmatrix} +\rho e_1 \\ -\rho e_2 \\ +\rho e_3 \\ \vdots \\ \pm \rho e_n \end{bmatrix} = \rho e_1 \qquad \text{(B-3)}$$

if e_2 , e_3, .., e_n = 0

The magnetic read system exhibits both the properties of homogeneity and additivity and is considered a linear system. Thus the principle of superposition holds, and data patterns can be constructed by the proper summing of isolated pulses.

VITA

John Popa

Candidate for the Degree of

Master of Science

Thesis: DESIGN TECHNIQUES FOR THE SATURATION MAGNETIC RECORDING PROCESS

Major Field: Electrical Engineering

Biographical:

Personal Data: Born in Akron, Ohio, December 3, 1923, the son of George Alexe, and Mary Popa.

Education: Attended grade school in Akron, Ohio; graduated from Garfield High School, Akron, Ohio in June, 1941; attended Lafayette College, Easton, Pennsylvania; received the Bachelor of Electrical Engineering degree from the University of Akron in June, 1949; enrolled in off-campus master's program at the Purdue University Center, Ft. Wayne, Indiana, 1953-1956; enrolled in off-campus master's program at the Syracuse University Center, Rome, New York, 1962; completed requirements for the Master of Science degree at Oklahoma State University in May, 1972.

Professional Experience: Design Engineer for General Electric Company, Fort Wayne, Indiana, and Waynesboro, Virginia, 1949 to 1961; Analytical Engineer for General Electric Company, Utica, New York and Oklahoma City, Oklahoma, 1961 to 1966; Senior Magnetics Engineer for General Electric Company, Oklahoma City, Oklahoma, 1966 to 1970; Senior Magnetics Engineer for Honeywell Information Systems Incorporated, Oklahoma City, Oklahoma, 1970 to present.

Professional Organizations: Senior Member, The Institute of Electrical and Electronics Engineers, Inc.; Registered Professional Engineer, the state of Oklahoma; Registered Professional Engineer, the state of Indiana.